arXiv:nucl-ex/0509018v1 14 Sep 2005

Measuring the Neutron's Mean Square Charge Radius Using Neutron Interferometry

F. E. Wietfeldt, M. Huber
Tulane University, New Orleans, LA

T. C. Black
University of North Carolina, Wilmington, NC

H. Kaiser
Indiana University Cyclotron Facility, Bloomington, IN

M. Arif, D. L. Jacobson, S. A. Werner
National Institute of Standards and Technology, Gaithersburg, MD

Abstract

The neutron is electrically neutral, but its substructure consists of charged quarks so it may have an internal charge distribution. In fact it is known to have a negative mean square charge radius (MSCR), the second moment of the radial charge density. In other words the neutron has a positive core and negative skin. In the first Born approximation the neutron MSCR can be simply related to the neutron-electron scattering length b_{ne}. In the past this important quantity has been extracted from the energy dependence of the total transmission cross-section of neutrons on high-Z targets, a very difficult and complicated process. A few years ago S. A. Werner proposed a novel approach to measuring b_{ne} from the neutron's dynamical phase shift in a perfect crystal close to the Bragg condition. We are conducting an experiment based on this method at the NIST neutron interferometer which may lead to a five-fold improvement in precision of b_{ne} and hence the neutron MSCR.

1 Introduction

The neutron has zero net electric charge, but it is composed of charged quarks so it may have an internal charge distribution. If so the neutron will interact electrostatically with other charged particles such as electrons. In a scattering experiment it is useful to parameterize the neutron charge distribution using the Sachs electric form factor $G_E(Q^2)$, the spatial Fourier transform of the neutron charge density in the Breit (brick wall) frame, *i.e.* in the frame where the neutron's initial momentum is $\boldsymbol{p}_i = -\boldsymbol{Q}/2$ and its final momentum is $\boldsymbol{p}_f = +\boldsymbol{Q}/2$ [1]. Writing the electric form factor as a multipole expansion in Q^2 we have:

$$G_E(Q^2) = q_n - \frac{1}{6}\langle r_n^2\rangle Q^2 + \ldots \tag{1}$$

At $Q^2 = 0$ the electric form factor is simply the neutron's net charge: $q_n = 0$. In the low Q^2 limit $G_E(Q^2)$ is dominated by the second term which contains the neutron mean square charge radius (MSCR) $\langle r_n^2\rangle$, the second moment of the neutron charge density:

$$\langle r_n^2\rangle = \int \rho(r) r^2 d^3r. \tag{2}$$

From (1) we see that $\langle r_n^2\rangle$ determines the slope of the form factor at $Q^2 = 0$:

$$\langle r_n^2\rangle = -6\frac{dG_E(Q^2)}{dQ^2}\Big|_{Q^2=0}. \tag{3}$$

In the subfield of nuclear physics concerned with understanding nucleon structure, one measures $G_E(Q^2)$ as a function of Q^2 by scattering electrons from light nuclei at various energies and compares it to the predictions of theoretical models. For this program (3) is an important constraint on the shape of $G_E(Q^2)$.

Theoretically there are several ways of understanding how a nonzero $\langle r_n^2 \rangle$ might arise. The simple SU(6) quark model predicts $G_E(Q^2)$ to be identically zero, and hence $\langle r_n^2 \rangle = 0$ [2]. The known $\Delta - n$ mass splitting implies a spin-dependent quark interaction that breaks SU(6) symmetry. Such a force would also tend to pull the up quark to the center of the neutron and push the down quarks to the edge, producing a nonzero $G_E(Q^2)$ and specifically a negative $\langle r_n^2 \rangle$ [3]. In another picture every neutron spends part of its time as a virtual proton-pion pair [4]. In this state the lighter π^- orbits the heavier proton, making a negative $\langle r_n^2 \rangle$. Recent theoretical efforts to calculate $\langle r_n^2 \rangle$ produce a negative sign but a large uncertainty on its magnitude [5, 6, 7].

In an experiment, the total coherent scattering length for neutron-atom scattering (far from any resonances and neglecting small effects such as the neutron's electric polarizability) is given by:

$$b_{\rm coh} = b_N + Z\,[1 - f(\boldsymbol{q})]\,b_{ne} \tag{4}$$

where b_N is the nuclear scattering length and b_{ne} is the neutron-electron scattering length, responsible for the electrostatic interaction between the neutron and a charged particle (*e.g.* electron). The first term in brackets corresponds to the nuclear electric charge and the second term to the atomic electrons. The form factor $f(\boldsymbol{q})$ is the spatial Fourier transform of the atomic electron charge distribution for momentum transfer $\boldsymbol{q}$.

The net charge of the particle and its internal charge distribution both contribute to b_{ne}. For neutron-atom scattering at low momentum transfer the second term in (1) dominates. From scattering theory, using the 1$^{\rm st}$ Born approximation, one obtains:

$$\langle r_n^2 \rangle = 3\,a_0 \left(\frac{m_e}{m_n}\right) b_{ne} = \ (86.34\ {\rm fm}) \cdot b_{ne}. \tag{5}$$

In recent experimental determinations of b_{ne}, total transmission cross sections are measured for epithermal and thermal neutrons on lead and bismuth targets [8, 9, 10]. These studies, and also the earlier work of Krohn and Ringo [11] using noble gas targets, contribute to the Particle Data Group's recommended value of $\langle r_n^2 \rangle = -0.1161 \pm 0.0022$ fm^2 [12]. This includes a scale factor of 1.3 to account for a minor disagreement. There is a much larger and still unexplained disagreement between measurements of b_{ne} from transmission measurements and older determinations neutron diffraction on crystals [13].

2 A New Method

Recently S. A. Werner proposed a new approach for a precision measurement of b_{ne} using neutron interferometry. The basic experimental setup is illustrated in Figure 1, which shows a standard LLL perfect crystal silicon neutron interferometer and the usual phase flag (*e.g.* fused silica). The neutron beam is split into two paths by Bragg diffraction, and the relative phase shift caused by different path lengths in the phase flag produces interference fringes in the neutron counters C_2 and C_3. Detailed introductions to the theory and operation of neutron inteferometers can be found in [14, 15, 16]. A separate perfect crystal silicon sample, cut from the same ingot as the interferometer, is placed across both downstream paths. This sample can be rotated about all three axes. It is

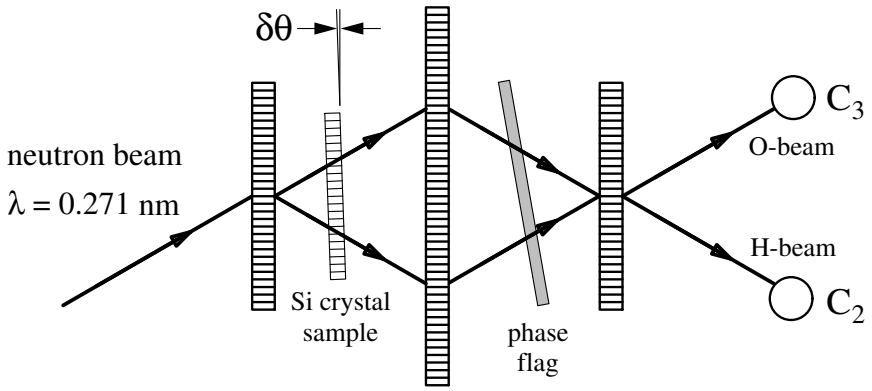

Figure 1: A sketch of the experimental setup.

aligned precisely to the Bragg condition (parallel to the interferometer blades) and then rotated by a small misset angle $\delta\theta$ as indicated. The neutron phase as a function of $\delta\theta$ over a range of ± 10 arcsec from Bragg is then measured.

Very close to Bragg the neutron obtains a *dynamical* phase shift that originates from the transition to the α and β solutions for the internal wave vector. According to dynamical diffraction theory this is given by [17]:

$$\Phi_{\rm dyn} = \frac{\nu_H}{\cos\theta_B}\left(-y \pm \sqrt{1+y^2}\right) D \tag{6}$$

where the minus (plus) sign corresponds to the α (β) solution. Here ν_H is the probability for Bragg scattering per unit path length, related to the crystal structure function F_H for this reflection by $\nu_H = F_H \lambda / V_{\rm cell}$. The parameter y is a scaled misset angle:

$$y = \frac{k \sin\theta_B}{2\,\nu_H}\delta\theta, \tag{7}$$

D is the crystal thickness, and θ_B is the Bragg angle. Because the crystal sample extends through both beam paths the kinematic phase cancels and the dynamical phase adds, producing a net relative phase:

$$\Delta\Phi = \frac{\nu_H}{\cos\theta_B}\left(y \pm \sqrt{1+y^2}\right) D \tag{8}$$

with the plus (minus) sign corresponding to positive (negative) misset angles. A plot of $\Delta\Phi$ *vs.* $\delta\theta$ is shown in Figure 2.

The sample crystal is suspended on a shaft connected to a 10 cm lever, which is moved by a self-calibrated PZT nanopositioner that steps over a range of 25 μm with 0.1 nm precision (P-753, Physik Instrumente, Karlsruhe, Germany [18]). The shaft rotates on a nylon flexure bearing, there are no sliding or rolling contacts, so the crystal rotates smoothly and the misset angle can be measured to 10^{-4} arcsec.

The neutron interferometer can measure the net relative phase shift $\Delta\Phi$ to within 1° in a single interferogram (in about 1000 s) The silicon lattice constant, neutron wavelength, and crystal thickness D are all known at the 10^{-5} precision level. Therefore by fitting the measured phase shift as a function of misset angle to Equation 8 one can with some effort determine ν_H, and hence F_H,

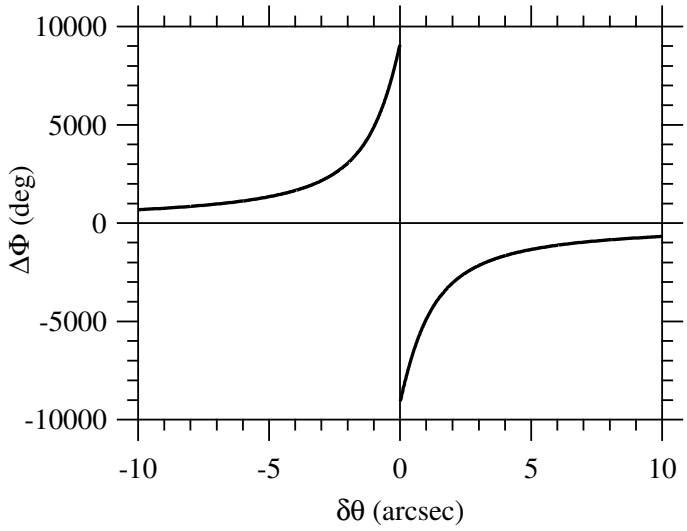

Figure 2: The theoretical relative phase $\Delta\Phi$ as a function of the misset angle $\delta\theta$ from Bragg, calculated from Equation 8.

to an absolute precision of about 3×10^{-5}. Near the Bragg condition the structure factor is related to the coherent scattering length (see 4) by:

$$F_H = \sqrt{32}\,(b_N + Z\,[1 - f(\boldsymbol{H})]\,b_{ne})\,. \tag{9}$$

In our case $f(\boldsymbol{H}) = 0.7526$ [19] is the form factor calculated for the reciprocal lattice vector $\boldsymbol{H}$ corresponding to the (111) reflection in silicon. In Equation 9, b_N is about 240 times larger than $Z\,[1 - f(\boldsymbol{H})]\,b_{ne}$. By rotating the crystal off Bragg far enough that the dynamical phase is negligible we can measure b_N *in situ* with a relative uncertainty of less than 10^{-5}, limited only by the uncertainty in the phase measurement, and subtract it from Equation 9. This will allow a determination of b_{ne} and hence $\langle r_n^2 \rangle$ with a net uncertainty of about 0.7%, more than a factor of three improvement from the present accepted value, and using a technique systematically much different from other precision measurements. If the experiment with silicon is successful we may repeat it using a perfect germanium crystal, improving the sensitivity by the increase in Z: a factor of 2.3. This may lead to a 0.3% measurement of b_{ne} and $\langle r_n^2 \rangle$, more than a factor of five improvement.

We note that this method is related to the experiment of Shull which first demonstrated Pendellösung interference fringes in neutron dynamical diffraction [20]. The structure factor F_H was precisely determined from the fringe separation and $b_{\rm coh}$ was obtained for the (111) reflection in silicon via Equation 9. The main advantages of our approach are (1) an improved overall precision due to the interferometric measurement of the neutron phase and (2) the ability to make a relative subraction of b_N from Equation 9 *in situ*.

References

[1] R. G. Sachs, Phys. Rev. **126**, 2256 (1962).

[2] R. Carlitz, S. D. Ellis, and R. Savit, Phys. Lett. B **64**, 85 (1976).

[3] N. Isgur, G. Karl, and R. Koniuk, Phys. Rev.D, **23**, 163 (1981).

[4] E. Fermi and L. Marshall, Phys. Rev. **72**, 1139 (1947).

[5] F. Cardarelli and S. Simula, Phys. Rev. C **62**, 065201 (2000).

[6] V. A. Karmanov, Nucl. Phys. A **699**, 148c (2002).

[7] W. R. B. de Araújo, *et al.*, Int. J. Mod. Phys. A **18**, 5767 (2003).

[8] Yu. Alexandrov, *et al.*, Sov. J. Nucl. Phys. **44**, 900 (1986).

[9] L. Koester, *et al.*, Phys. Rev. C **51**, 3363 (1995).

[10] S. Kopecky, *et al.*, Phys. Rev. C **56**, 2229 (1997).

[11] V. E. Krohn and G. R. Ringo, Phys. Rev. D **8**, 1305 (1973).

[12] S. Eidelman *et al.* (Particle Data Group), Phys. Lett. B **592**, 1 (2004) and 2005 partial update (URL: http://pdg.lbl.gov).

[13] Yu. Alexandrov, *et al.*, Sov. J. Nucl. Phys. **20**, 623 (1975).

[14] V. F. Sears, *Neutron Optics*, Oxford University Press (1989).

[15] H. Kaiser and H. Rauch, *De Broglie wave optics: neutrons, atoms and molecules*, in Bergmann/Schaefer Optics of Waves and Particles, Walter de Gruyter Verlag (1999).

[16] H. Rauch and S. A. Werner, *Neutron Interferometry*, Oxford Science Publications (2000).

[17] *ibid.*, pp. 294–303.

[18] Certain trade names and company products are mentioned in the text or identified in illustrations in order to adequately specify the experimental procedure and equipment used. In no case does such identification imply recommendation or endorsement by the National Institute of Standards and Technology, nor does it imply that the products are necessarily the best available for the purpose.

[19] D. T. Cromer and J. B. Mann, Acta Cryst. A **24**, 321 (1968).

[20] C. G. Shull, Phys. Rev. Lett. **21**, 1585 (1968).